JOURNAL OF APPLIED ELECTROCHEMISTRY 7 (1977) 95–106

Structural, electrical and electrochemical characterization of Ni-Pr oxide thick films

C. MARI, V. SCOLARI, G. FIORI, S. PIZZINI*

Electrochemistry and Metallurgy Institue, University of Milan, via Venezian 21, Milano, Italy

Received 13 April 1976

Oxides with metallic conductivity could and have been used instead of noble metals as insert electrodes in aqueous solutions as well as electrodes for high temperature fuel cells and electrolysers and as catalysts for the conversion of exhaust gases from internal combustion engines. The aim of this paper is to report the results of a physico-chemical characterization (structure, morphology, electrochemical behaviour) of Ni–Pr oxides which have been proposed as electrode materials for high temperature fuel cells.

The electrochemical characterization was carried out in aqueous solutions at room temperature and with solid electrolytes at high temperature. Evidence has been found in the former case for an oxide electrode type of behaviour. In the high temperature case, very low overvoltage values have been observed during cathodic oxygen reduction, while the electrode undergoes a reaction with oxygen during anodic oxygen evolution.

1. Introduction

Platinum, on account of its outstanding chemical and physical properties in oxidizing environments at high temperature, has found widespread applications as an electrode material.

It is well known, for example, that porous platinum is used as the material for oxygen electrodes at high temperatures, both in the case of oxygen sensors [1–3] and in the case of electrochemical oxygen pumps [4–6]. Its high cost, the fact that the original porous structures gradually deteriorate with time due to sintering, and that oxygen solubility and diffusivity in platinum is negligible, which leads to irreversibility effects under moderate electrical loads, are all circumstances which favour the alternative use of oxides.

Amongst other properties, in order to be used as substitutes for platinum, metallic oxides should either be prepared with a well-defined porous structure, which favours the oxygen exchange at the electrolyte–metallic oxide–gas phase boundary or should exhibit good oxygen chemical diffusivity values, which favour a fast transport of oxygen from or to the gaseous phase and to the electrolyte.

As possible substitutes for platinum, oxides with the fluorite structure which exhibit enhanced oxygen diffusivity, and oxides with the rutile or perowskite structure which exhibit metallic conductivity, are the favourites. It is the aim of this paper to report and discuss the results of a structural and physico–chemical characterization of nickel praseodymium mixed oxide films which have been used in the past [7] as the electrode material for oxygen electrodes in high temperature fuel cells and electrolysers, but which could be eventually used as the electrode material for conventional applications of wet electrochemistry.

2. Experimental

2.1. *The preparation of $NiPr_2O_4$ powder*

An oxide of nominal composition $NiPr_2O_4$ was prepared starting from anhydrous $PrCl_3$ which was converted to the nitrate before mixing it with an aqueous solution of $Ni(NO_3)_2$ in the proper ratio. The solution was then dried and the nitrates decomposed to a brownish-black powder at 300–500° C before firing it at 1100–1300° C for the completion of the reaction. The extent of the

* Present address: Material Science Dept., Istituto 'G. Donegani', Novara, Italy.

Table 1. Experimental and calculated X-ray data of $NiPr_2O_4$ *powder*

D(Å)(obs)	D(Å)(calc)	I
3·663 8	3·664 9	80
3·113 9	3·113 6	65
2·818 3	2·816 9	100
2·728 3	2·721 9	87
2·413 7*	2·411 1	35
2·089 4*	2·088 9	85
2·076 2	2·075 7	60
2·052 2	2·057 5	70
2·038 3	2·041 1	70
1·917 1	1·917 3	85
1·816 5	1·820 0	50
1·706 9	1·706 8	23
1·652 1	1·653 6	35
1·644 7	1·644 2	37
1·632 7	1·632 6	45
1·614 3	1·613 9	62
1·591 5	1·589 9	75
1·578 6	1·584 2	75
1·557 2	1·556 8	20
1·477 5*	1·483 8	23
1·417 0	1·417 3	15
1·364 0	1·360 9	20
1·352 2	1·351 7	20
1·347 9	1·346 7	35
1·237 8	1·237 6	30
1·231 8	1·232 4	28
1·222 1	1·221 6	25
1·221 0	1·221 0	28
1·217 1	1·216 5	15
1·208 7	1·208 6	38
1·133 8	1·133 9	20
1·131 2	1·131 1	20
2·695 9		87
2·472 5		10
2·183 8		15
1·690 8		20
1·126 9		20

* These peaks could be also referred to NiO.
Direct lattice constants: a(Å) 3·864 57; b(Å) 3·834 77; c(Å) 12·455 41; α(deg) 90·000 00; β(deg) 90·654 15; γ(deg) 90·000 00.

reaction could be followed by means of X-ray powder diffraction measurements. After 42 h at 1300° C the X-ray diffraction patterns are invariant.

Table 1 reports the intensities and the values corresponding to the first 45 major diffraction lines. With the exception of five, the observed values agree with those of the $NiPr_2O_4$ structure, calculated from the known K_2NiF_4 structure. The five residual peaks refer to the $NiPrO_3$ phase, which is the major source of contamination of the $NiPr_2O_4$ phase.

2.2. *The preparation of* $NiPr_2O_4$ *films*

$NiPr_2O_4$ films on YSZ have been previously prepared [7] by means of a slurry of the fully reacted oxide which is suitably deposited onto the ceramic electrolyte. As preliminary experiments demonstrated that by this technique poorly adherent films could be obtained, a different procedure has been used throughout, which consists of preparing a concentrated aqueous solution of $Ni(NO_3)_2$ and $Pr(NO_3)_3$ of the proper composition which is then deposited at room temperature on the ceramic electrolyte. Both painted and sprayed deposits have been prepared, which are first dried and then fired at 500° C.

In order to obtain thick deposits (> 1 μm) this procedure must be repeated at least 20 times, when using a solution 0·15 mol dm^{-3}. The film is finally submitted to an annealing process at temperatures no higher than 1100° C for 2 h (in order to avoid sublimation and decomposition) which causes the completion of the reaction and consequently, the colour to turn to brilliant black.

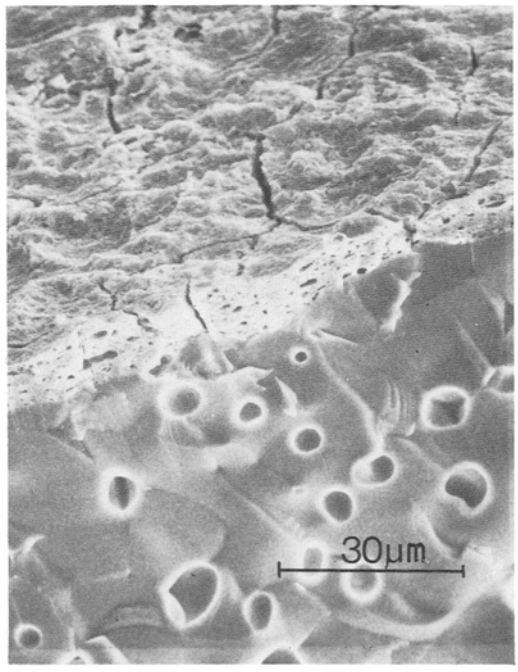

Fig. 1. Section of $NiPr_2O_4$ film on the solid electrolyte (S. E. M.).

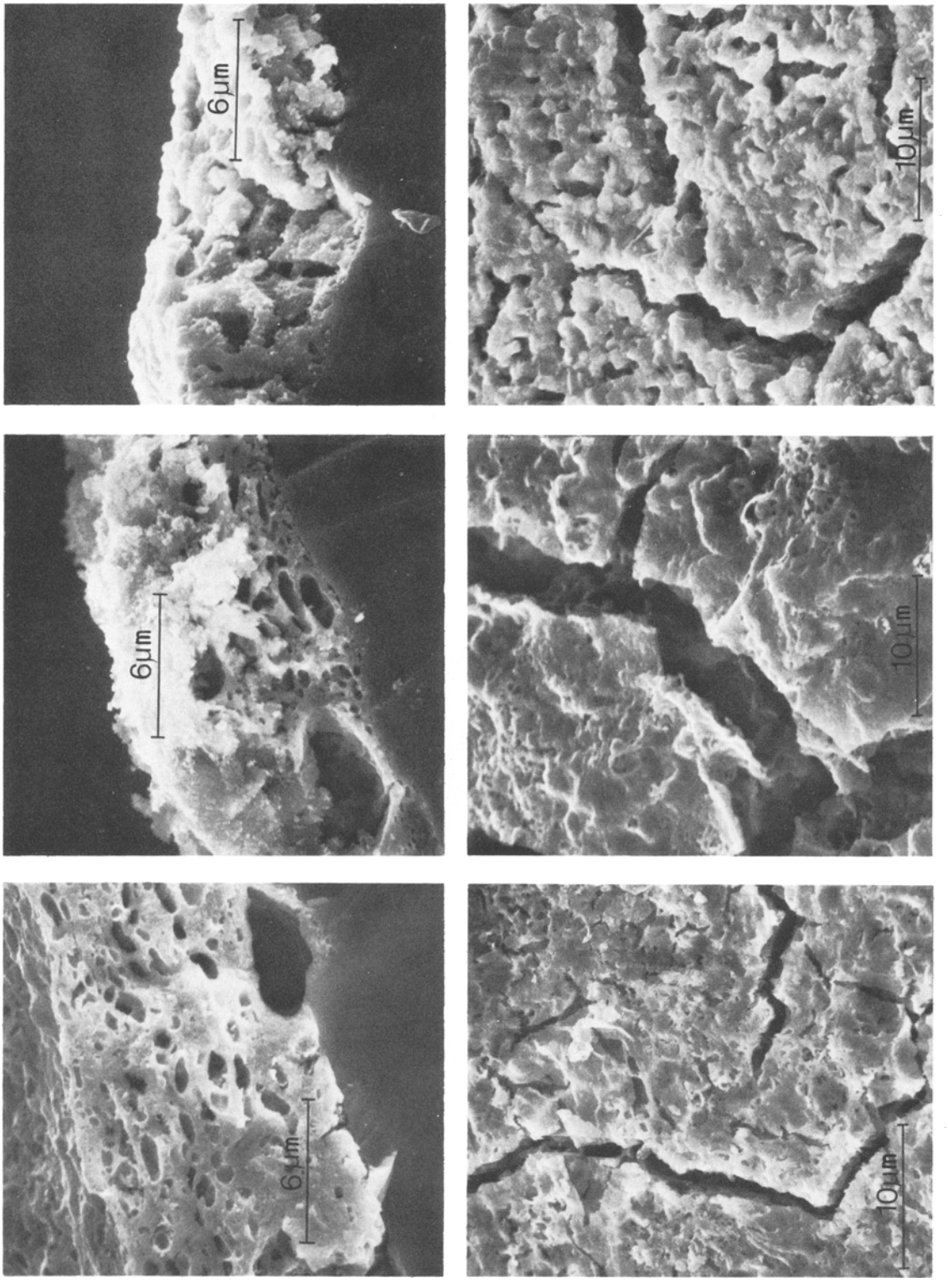

Fig. 2. Section and view of $NiPr_2O_4$ film, on the solid electrolyte, after annealing at 900, 1050 and 1100° C (S. E. M.).

The films, albeit being well-adherent to the substrate, are always fractured as it is apparent in Fig. 1, and have a characteristic Swiss–cheese porous structure with very few open pores. It has been shown that the film texture evolves with the temperature and that at the highest temperature (1100° C) a recrystallization process takes place (see Fig. 2) which leaves a micro-porous structure. As soon as the recrystallization process occurs, the electrical conductivity of the film rises appreciably.

2.3. *The deposition of $NiPr_2O_4$ films on platinum foils*

Films suited for the electrochemical characterization of the mixed oxide in aqueous solutions were prepared by similar procedures to those described above by using as the substrate a sheet of platinum since electrodes deposited on a ceramic (ZrO_2 or Al_2O_3) substrate did not exhibit reproducible behaviour.

It has been shown that an essential precaution for obtaining a film with a good morphology is to carry out the decomposition of the nitrates and the subsequent annealing in an homogeneous temperature environment. X-ray powder diffraction patterns of these films are similar to those of the corresponding powders.

3. Electrochemical properties

3.1. *Cathodic and anodic polarization measurements at high temperatures*

$NiPr_2O_4$ films deposited on a tube of YSZ which serves as the electrolyte were cathodically and anodically polarized by using the cell and the apparatus already described [8]. In order to obtain a homogeneous distribution of the current along the entire electrode/electrolyte interface, a technique similar to that employed for silicon solar cells has been used. The electrical contacts were realized by means of a platinum net obtained by depositing (with a mask) and firing a platinum paste on to the oxide film.

While anodic polarizations were carried out in a range of oxygen pressures which varied from 1–3 x 10^{-6} bar, cathodic polarization experiments were restricted to the 1–5 x 10^{-2} bar range. The reproducibility of the results was generally good, in the sense that when using the same electrode,

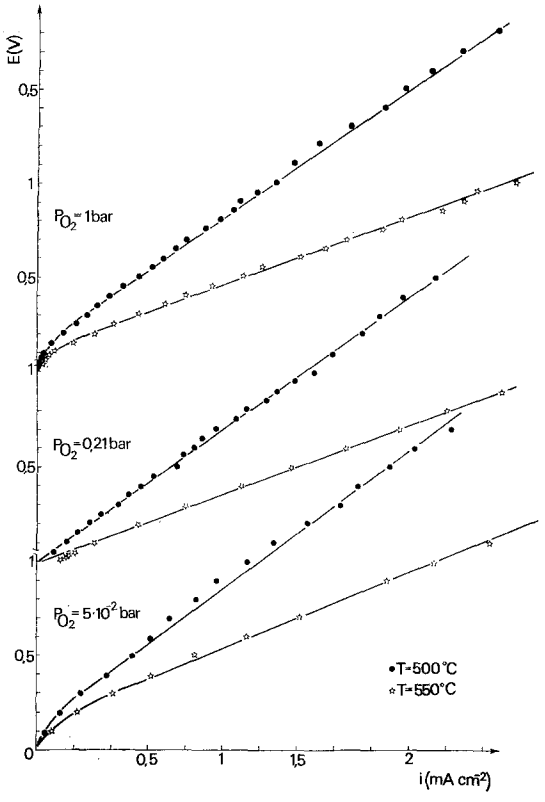

Fig. 3. Current–voltage curves for cathodic polarization of $NiPr_2O_4$ electrodes.

the results could be obtained repetitively. However, differences in the absolute values of the overvoltage were observed if the electrode and the electrolyte tube were changed.

Figs. 3–5 show the results of cathodic polarization measurements. It is apparent that at temperatures as high as 700° C overvoltage contributions are present, whereas at the higher temperatures the current–voltage curves appear to be entirely ohmic in character.

It should be noted that negligibly low overvoltage contributions are also observed at lower temperatures for the 0·21 bar isobars. We could interpret this effect by considering that the oxide films have been prepared by annealing and thereafter cooling in air the products of thermal decomposition of a nitrate mixture. We assume therefore that in this case the composition of the film has been adjusted to that corresponding with the equilibrium conditions between the solid phase and the atmosphere.

When the oxide film is used as an electrode in different conditions, the compositional modifica-

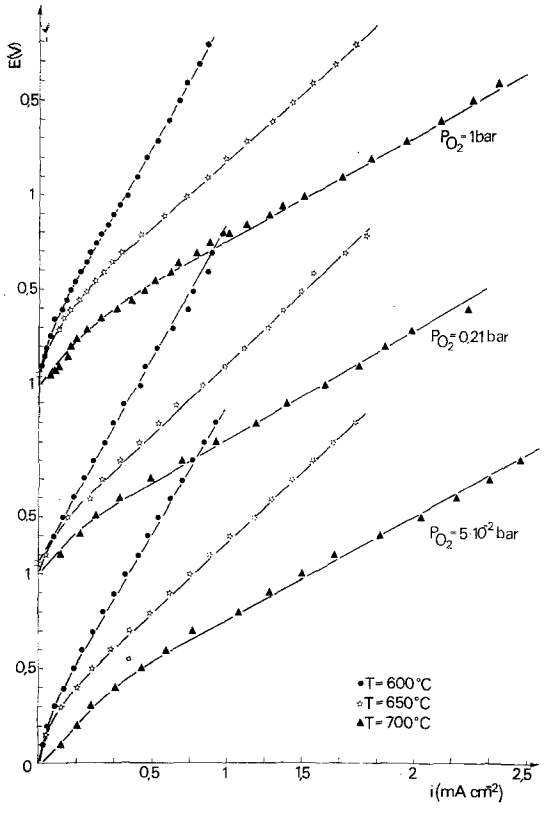

Fig. 4. Current–voltage curves for cathodic polarization of $NiPr_2O_4$ electrodes.

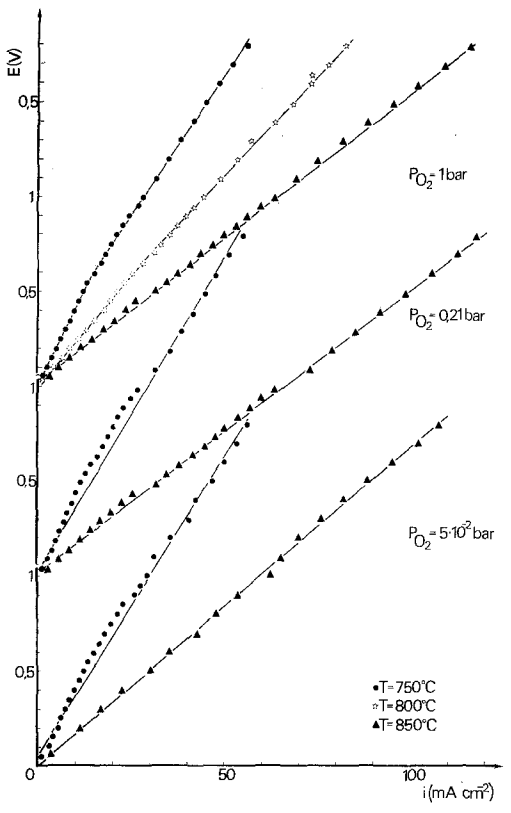

Fig. 5. Current–voltage curves for cathodic polarization of $NiPr_2O_4$ electrodes.

tions which intervene during the cathodic polarization are reflected by the onset of overvoltage contributions. The activation energy calculated from the slopes of the linear parts of the current–voltage curves corresponds to the activation energy of the ionic conductivity of the electrolyte measured by a.c., thus indicating that the electrode reaction occurs reversibly and that the overall rate of the electrochemical process is limited by the oxygen ion transport in the electrolyte.

The results of anodic polarization measurements are reported in Figs. 6 and 7.

It is apparent that whereas at low temperatures overvoltage contributions appear, at high temperatures an active–passive type of transition occurs which would correspond to the oxidation of the electrode material with the formation of a new phase. When one considers the slopes of the E versus I curves before and after the active–passive transition (see Fig. 7), one recognizes that at any temperature, but especially at the lowest ones the electrode resistivity decreases as soon as the transition has occurred.

3.2. *Electrochemical behaviour of $NiPr_2O_4$ electrodes in aqueous solutions*

The electrochemical behaviour of $NiPr_2O_4$ electrodes has also been examined in aqueous solution in the range of temperatures between 20 and 60° C. In this case both the rest potentials and the current–voltage curves have been measured as functions of the pH of the solutions. Some values of the rest potential in standard buffer solutions measured against a SCE are reported in Fig. 8 as a function of the pH.

As in the case of many metal/metal oxide electrodes [9], where the chemical potential of oxygen is fixed by the coexisting phases, and of non-stoichiometric oxide electrodes such as RuO_2 [10] and $NiLa_2O_4$ [11], the rest potentials of the $NiPr_2O_4$, electrode were shown to be stable and reproducible within 5–10 mV at pH values ranging between 7 and 13. Usually the time needed for obtaining equilibrium conditions was of the order of a few (not more than three) minutes.

In this pH range a linear dependence of the rest

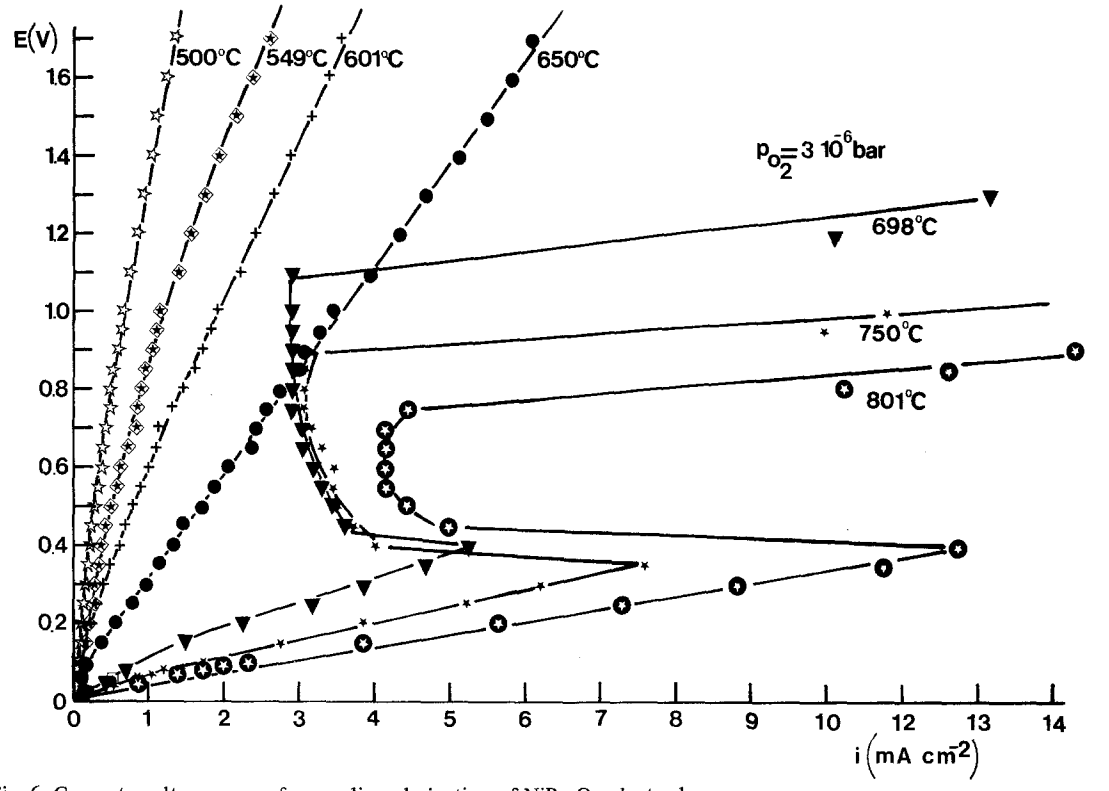

Fig. 6. Current–voltage curves for anodic polarization of $NiPr_2O_4$ electrodes.

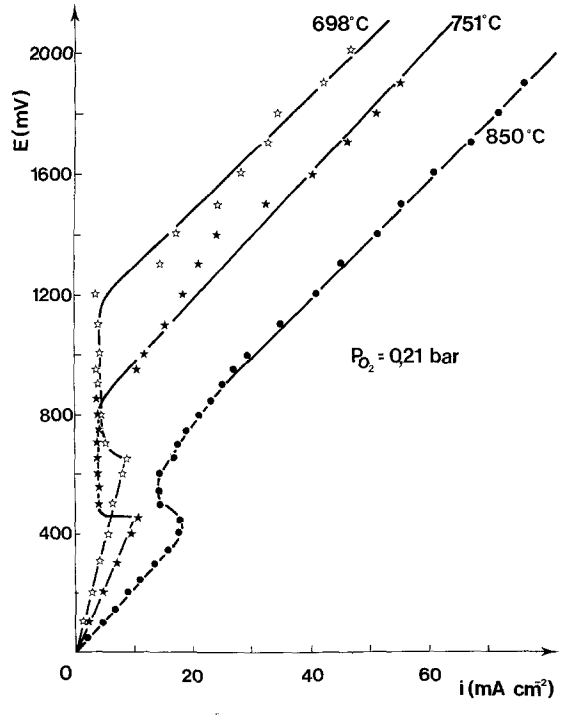

Fig. 7. Current–voltage curves for anodic polarization of $NiPr_2O_4$ electrodes.

potentials on the pH is observed, which could be expressed by the equation:

$$E(\text{mV}) = 710 - 59{\cdot}16\ \text{pH at } 25^\circ\text{C}\ (7 \geqslant \text{pH} \geqslant 13)$$

where 710 is the value (in V) of the standard electrode potential E^0. As irreversible degradation of the electrode occurs at pH values lower than 6, the E^0 value could however only be obtained by linear extrapolation to a pH value equal to zero.

The current–voltage characteristics have also been determined by means of the potential sweep technique applied between − 200 mV and the potential of oxygen evolution. Various sweep rates (1–50 mV s^{-1}), NaOH concentrations (0·1–3 mol dm^{-3}) and temperatures (20–60° C) have been employed.

The experimental apparatus consisted of a conventional three-compartment cell where the $NiPr_2O_4$ electrode was the working electrode: a platinum wire was used as the counter electrode and a SCE as the reference electrode. The temperature was controlled by means of an air thermostat to ± 1° C.

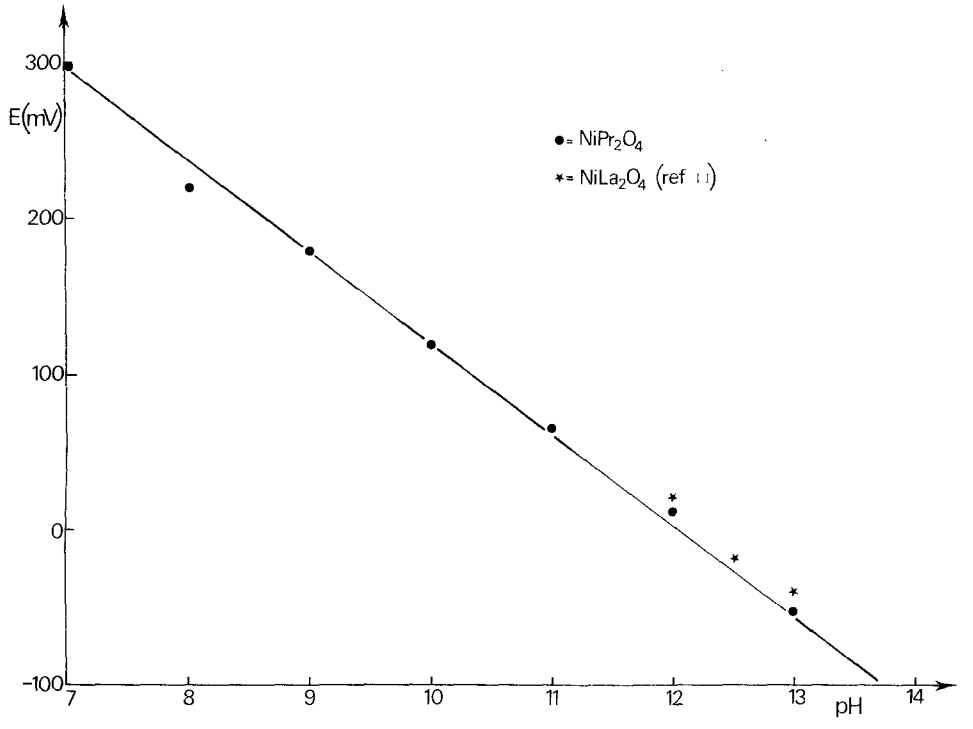

Fig. 8. Static-potential values against pH values at 25° C.

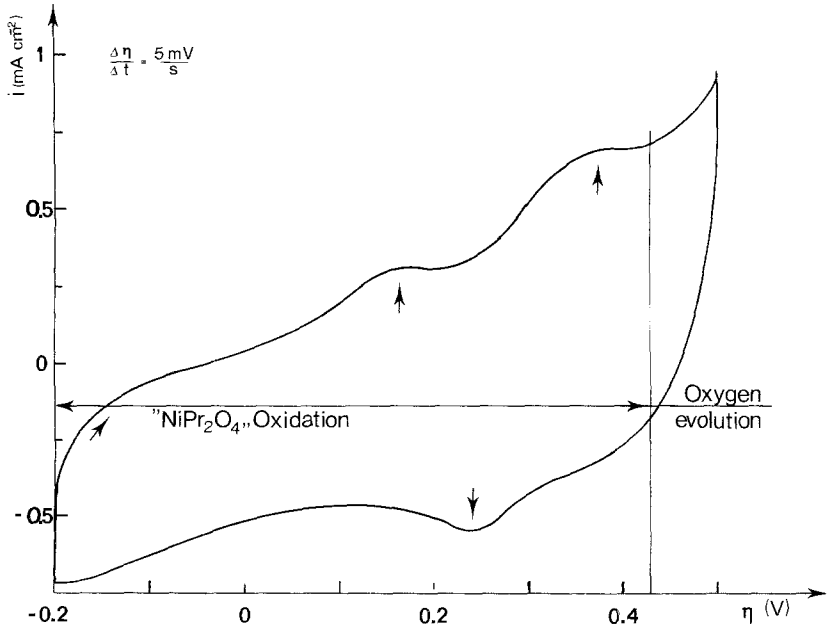

Fig. 9. Cyclic voltammogram in 1 N NaOH solution at 25° C. Freshly prepared electrode.

Figs. 9 and 10 report two potential sweeps obtained under the same experimental conditions (NaOH 1 mol dm^{-3}, $T = 25°$ C, sweep rate 5 mV s^{-1}). The first one is characteristic either of freshly prepared electrodes or, alternatively, of electrodes on which anodic oxygen discharge was never allowed to occur. The second one has been obtained with an electrode which was previously

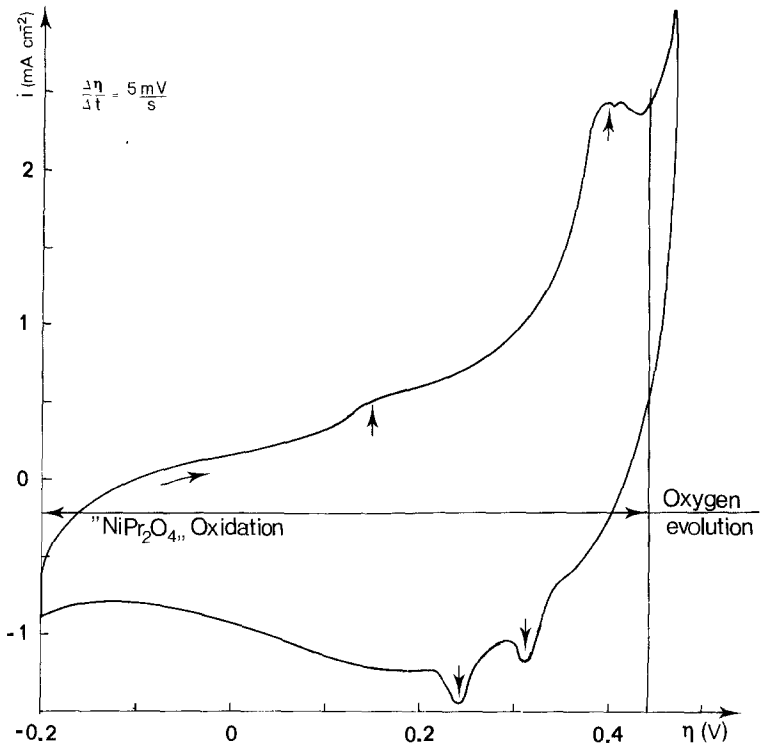

Fig. 10. Cyclic voltammogram in 1 N NaOH solution at 25° C. Electrode used to study oxygen evolution.

used to study oxygen evolution. These behaviours are characteristic of the above described conditions and are reasonably reproducible with different electrodes. Experiments carried out at higher temperatures do not present significant differences.

For a proper analysis of these results it appears worthwhile to distinguish two voltage regions (whose relative extents are shown to depend on the pH) which correspond, respectively, to the oxidation of the working electrode material and to the anodic oxygen evolution. The results refering to the first region are very difficult to interpret because the electrode behaviour is a function not only of the electrolyte concentration, temperature and sweep rate but also of the previous history of the electrode.

Two oxidation peaks (one at 200 mV versus the SCE and one at 350 mV versus the SCE) were observed both in the case of freshly prepared electrodes and in the case of electrodes already polarized up to the oxygen discharge. It is , however, apparent that the current corresponding to the second peak is lower for freshly prepared electrodes and that during the reduction cycle a new peak appears when oxygen discharge has been allowed to occur on the electrode. Finally the dependence of the E_p values on the concentrations of the OH^- ions has been determined as 60 mV dec^{-1} for the second and 110–120 mV dec^{-1} for the third peak.

The results refering to the oxygen evolution region show that a large current range exists where Tafel conditions are fulfilled, independently of the previous history of the electrode and of the sweep rate. In Fig. 11 the Tafel plots at various pH values are reported. The values of the b coefficient are nearly equal and correspond to 120 ± 10 mV. Apparently, this slope value corresponds to that observed with platinum electrodes in alkaline solutions in the same current density range [9]. In Fig. 12 the electrochemical reaction order has been evaluated at various values of overvoltage $(\delta \log i/\delta \log C)_\eta$ and it is shown to be equal to 0·6. With regard to the dependence of the overvoltage on the pH, it can be deduced from Fig. 13 that the slope $(\delta \log \eta/\delta \log C)_i$ equals 0·6.

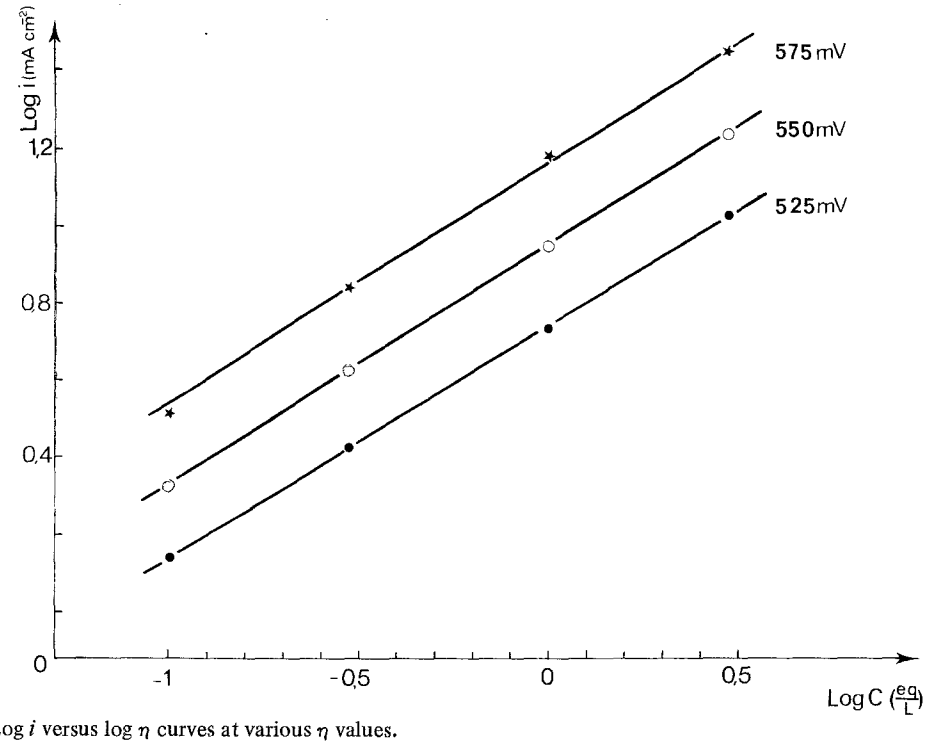

Fig. 11. Log i versus log η curves at various η values.

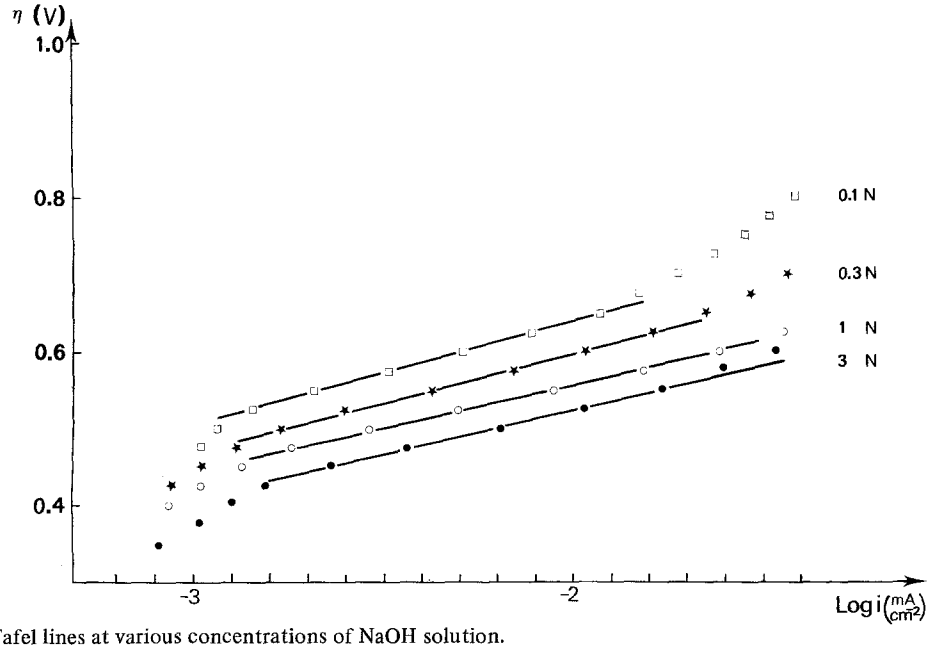

Fig. 12. Tafel lines at various concentrations of NaOH solution.

4. Discussion

Compared with platinum electrodes and other oxide electrodes at high temperatures (see Table 2), $NiPr_2O_4$ electrodes present a remarkably better cathodic performance but a very complicated anodic behaviour. The reversible behaviour of $NiPr_2O_4$ electrodes under cathodic polarization can be understood if catalytically enhanced oxygen reduction takes place at the YSZ/$NiPr_2O_4$

Table 2. Anodic and cathodic behaviour on metallic and oxide electrodes at high temperatures

Type of electrode	*Temperature* (° C)	*Anodic performance*	*Cathodic performance*	*Remarks*	*References*
Pt	$T < 800$	Slight overvoltage which decreases under heavy anodic polarization ($i > 3$–4 mA cm^{-2}).	Diffusion limited currents, relatively high overvoltage	Under anodic polarization Pt oxide film occurs	12, 13
	$T > 800$	Ohmic behaviour, no overvoltage			
RuO_2	820	Activation overvoltage controlled (Tafel plots between 0·1 and 10 mA cm^{-2})	Reversible behaviour (no overvoltage) at atmospheric pressure. At an oxygen partial pressure $\leqslant 10^{-2}$ the electrode decomposes to Ru metal under cathodic polarization.	Under strong O_2 evolution the volatilization of RuO_2 takes place through gaseous RuO_3 or RuO_4	12
V_2O_5	500–575	Slight overvoltage at the lowest temperatures, reversible behaviour at 500° C, and 1 atm O_2	Slight overvoltages at $T < 575$° C	At $P_{O_2} < 1$ atm the overvoltage increases.	12
$CeO_2 - x$	1000	Reversible behaviour up to 2 mA cm^{-2} for stoichiometric electrodes up to 0·7–0·8 mA cm^{-2} when $x = 0{\cdot}13$ (CO/CO_2 atm)	Not measured	As diffusion coefficients of O_2 in non-stoichiometric oxide are higher than in the stoichiometric one, the rate determining step should be a slow chemical reaction	14
$NiPr_2O_4$	700–900	Reversible behaviour after the electrode has undergone an active–passive transition (oxidation to $NiPrO_3$?)	Reversible behaviour up to 100 mA cm^{-2} at $5{\cdot}10^{-2}$ bar P_{O_2} and 850° C		This work

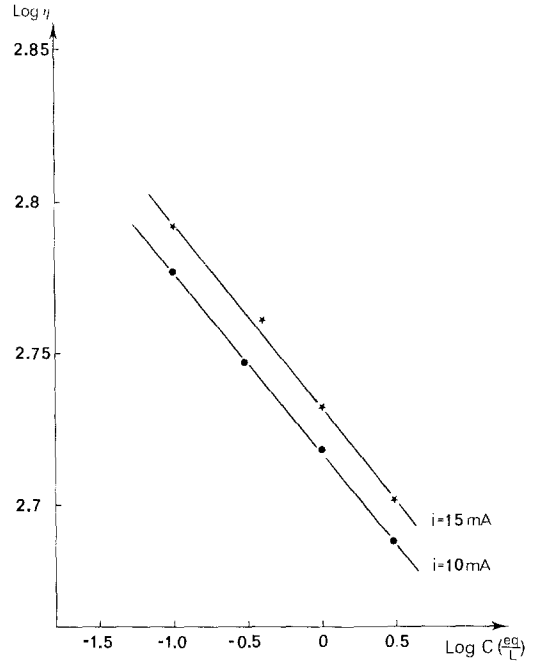

Fig. 13. Log η versus log C curves at various i values.

interface and fast molecular diffusion of oxygen through the pores.

Fast diffusion of atomic oxygen across the oxide film can be assumed as a possible alternative source of reducible oxygen at the oxide/electrolyte interface. According to previous calculations [13], we expect a limiting current due to Knudsen diffusion through the pores at 100 mA cm^{-2}, for a porous film electrode similar to that used in the present experiments, having a pore size intermediate between 0·01 and 0·1 μm, in the case of molecular diffusion of oxygen through the pores. The fact that the anodic overvoltage turns out to be negligible after the electrode has undergone an active–passive transition which we attribute to the oxidation of $NiPr_2O_4$

$$NiPr_2O_4 + \tfrac{1}{2}O_2 \rightarrow NiPrO_3 + PrO_{1.5} \quad (1)$$

$$NiPr_2O_4 + O_2 \rightarrow NiPrO_3 + PrO_2, \quad (2)$$

indicates that both $NiPr_2O_4$ and $NiPrO_3$ are catalytically active materials, while $PrO_{1.5}$ or PrO_2 allow fast transport to the atmosphere of the anodically produced oxygen.

Due to this complication, it is hard to generalize the results of the present experiments. However, for a satisfactory behaviour under cathodic and anodic polarization, the electrode material chosen must be thermodynamically stable with respect both to the oxidation and the reduction reaction.

As soon as we consider the behaviour of the $NiPr_2O_4$ electrode at rest in aqueous solution, we recognize that it works as an oxide electrode, like the $NiLa_2O_4$ electrode already studied by Brenet [11]. As in this case, the electrode potential lies in the range of potentials characteristic of the $Ni(OH)_2/Ni(OH)_3$ couple and this finding is a good indication that the redox reactions at these electrodes involve primarily a change in the oxidation state of lattice nickel and that there is no apparent influence of platinum, coming from the platinum grid, which is eventually dissolved in the electrode during the high temperature treatment.

The fact that the electrode is actually a mixture of $NiPr_2O_4$ and $NiPrO_3$ (+ undetected traces of Pr-oxides) underlies the behaviour of the $NiPr_2O_4$ electrode at rest, the chemical potential of oxygen being constant, as in the case of metal/metal oxide electrodes. On this basis, and that of the experimental reaction order, the values of the b coefficient and the pH dependence of the overvoltage, it is apparent [15] that the rate limiting step for oxygen evolution is the electrochemical discharge of OH^- ions on a previously discharged radical, under conditions of Langmuir-type adsorption and with a degree of surface coverage close to one [15]. The transfer coefficient relative to the above-described experimental data is 0·5–0·6.

The oxygen evolution on $NiPr_2O_4$ would then follow a mechanism of the type:

$$NiPr_2O_4 + H_2O \leftrightarrows NiPr_2O_4(OH) + H^+ + e \quad \text{(fast)} \quad (3)$$

$$NiPr_2O_4(OH) + OH^+ \leftrightarrows NiPr_2O_4 \cdot O^* + H_2O + e \quad \text{(fast)} \quad (4)$$

where by O^* we mean an oxygen atom adsorbed at the surface.

$$NiPr_2O_4 \cdot O^* + OH^- \leftrightarrows NiPr_2O_4 \cdot O^*(OH) + e \quad \text{(slow)} \quad (5)$$

in which the first reaction represents formally the oxidation of Ni^{2+} to Ni^{3+}, whilst the second and third ones are the formal consecutive steps of the oxygen evolution reaction. From $NiPr_2O_4 \cdot O^*(OH)$ the oxygen would be then rapidly desorbed.

The activation energy in the Tafel region of the current–potential curves has also been determined; the value of 15 kcal mol^{-1} confirms that a chemical reaction is the rate limiting step.

Although we cannot take into account the true surface area of the electrode, it is apparent that the kinetic behaviour of $NiPr_2O_4$ electrodes towards anodic oxygen evolution is comparable with that of platinum. Unfortunately cycling of the electrode causes its irreversible degradation, which hinders some practical applications of this electrode.

Acknowledgements

The authors thank Mr G. Terzaghi and Mr Roberto Bonecchi (Centro Microscopia Elettronica, Politecnico di Milano) for their skilful help during the experimental work and Dr Shannon for the interpretation and discussion of the X-ray powder patterns. This work has been carried out with the support of CNR Research grant No. 71.01156.11. 115.A.17.

References

[1] J. Fouletier, H. Seinera and M. Kleitz, *J. Appl. Electrochem.* **4** (1974) 305.

[2] T. H. Etsell and S. N. Flengas, *Mat. Trans.* **3** (1972) 27.

[3] R. A. Rapp, 'Techniques of Metal Research' Vol. 4, Part. 2 Interscience, New York (1970) p. 123.

[4] D. Yanu and F. A. Kröger, *J. Electrochem. Soc.* **116** (1969) 594.

[5] J. Besson, C. Deportes and M. Kleitz, *Brevet. Francais No. Provisoire* 128327 (Nov. 1976): M. Kleitz, Thesis, Grenoble (1968) p. 49.

[6] L. Heyne, *Nat. Bur. of Standards Special Publication* no. 296 (Eds. J. B. Wachtman, Jr. and A. D. Franklin) (1968).

[7] S. P. Mitoff, private communication. For $LaCoO_3$ and $PrCoO_3$ see also H. S. Spacil and C. S. Tedmon, *J. Electrochem. Soc.* **116** (1969) 1627.

[8] S. Pizzini, M. Bianchi, A. Corradi and C. Mari, *J. Appl. Electrochem.* **4** (1974) 7.

[9] J. P. Hoare, 'The Electrochemistry of Oxygen', Interscience, New York (1968) p. 69.

[10] D. Galizzoli, F. Tantardini and S. Trasatti, *J. Appl. Electrochem.* **4** (1974) 57.

[11] H. Nguyen Cong, P. Charter and J. Brenet, *C. R. Acad. Sci. Paris*, Ser. C, **279** (1974) 1085.

[12] S. Pizzini, C. Mari, A. Corradi and F. Forti, *Polska Akad. Nauk. Ceramika* **21** (1974) 171.

[13] S. Pizzini, M. Bianchi, P. Colombo and S. Torchio, *J. Appl. Electrochem.* **3** (1973) 153.

[14] C. Riccardi, Thesis, Imperial College, London (1971).

[15] B. E. Conway, 'Theory and principles of electrode processes', Chap. 8, The Roland Press, New York (1965) pp. 174–5.